
Properties of Fluid Deuterium Under Double-Shock Compression to Several Megabars

The equation of state of hydrogen at pressures of a few megabars, temperatures of a few electron volts, and compressions of up to several times liquid density has been a source of ongoing experimental^{1–4} and theoretical^{5–11} controversy. Understanding the properties of hydrogen under such conditions is fundamental to the modeling of massive planets, brown dwarfs,¹² and inertial confinement fusion. At present, access to these dense, high-pressure states can be achieved only by using shock waves; Hugoniot measurements are thus the primary tool for constraining dense-hydrogen equation-of-state (EOS) models.

Determining the density of a shocked material with a compressibility as large as hydrogen requires high-precision measurements of the primary observables. This is because fractional errors in the inferred compression ratio ρ/ρ_0 are $\rho/\rho_0 - 1$ times greater than fractional errors in the observables U_s (shock speed) and U_p (particle speed). Making a measurement precise enough to discriminate between the various deuterium EOS models thus presents a significant experimental challenge.

The first experiments to study shocked deuterium above 0.2 Mbar on the principal (i.e., single-shock) Hugoniot used laser-driven shock waves and a new, absolute measurement technique—results showed five- to sixfold compression between 1 and 2 Mbar.¹ This was in general agreement with the linear-mixing model of Ross⁷ but was in significant disagreement with the original *SESAME* model developed by Kerley.⁵ Subsequent experiments using magnetically driven flyer plates and a relative measurement of U_p based on aluminum impedance matching, found slightly over fourfold compression at 0.4 Mbar, which decreased to fourfold compression at 0.7 Mbar and 1 Mbar.³ These data were consistent with a new *SESAME* model developed by Kerley⁸ (which, for clarity, we refer to as the Kerley98 model) and *ab initio* models^{10,11} but exhibit slightly higher compressibility than the original *SESAME*⁵ and significantly lower compressibility than the Ross model. Although the pressure range of these two experiments overlapped only slightly, a clear discrepancy emerged

near 1 Mbar. This discrepancy may indicate a lack of understanding of the fundamental processes in hydrogen. ICF target designs can readily accommodate these differences because they occur at relatively low pressures encountered early in the implosion. Astrophysical models, however, depend greatly on the precise details of EOS models to extrapolate conditions of large planetary bodies. This small difference can have huge effects.

The first experiment to study deuterium under double-shock conditions at megabar pressures was performed by Mostovych *et al.*,² who used shocks reflected from an aluminum anvil. They recognized that the expected differences between EOS model predictions for the experimental observables are greater in a reflected-shock measurement than in a single-shock measurement. Reflected shocks thus provide a more-sensitive experimental platform for discriminating between the various models; they do, however, probe not only the principal Hugoniot but also the re-shock Hugoniots and thus are a complementary, rather than an equivalent, probe of the equation of state. The data of Mostovych *et al.*,² taken up to single-shock pressures of 1.3 Mbar, had significant uncertainties, with error bars on a single point spanning the difference between the various models; on average, however, results agreed with the more-compressible linear-mixing model of Ross.

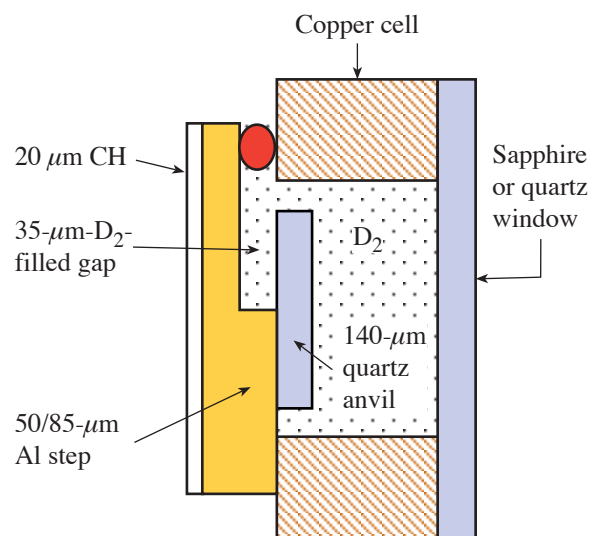
In this study we examine the behavior of fluid deuterium shocked initially to 0.7 to 2.5 Mbar and then double shocked to 2.5 to 9 Mbar. We cover a wider range of pressures than Mostovych *et al.*² and significantly improve upon the precision of those experiments by using α -quartz—a transparent re-shock anvil material—rather than aluminum. This allows us to use a high-precision, line-imaging optical interferometer to record the shock-front velocity continuously as it transits the deuterium–quartz interface. Such an approach also minimizes any systematic errors due to shock unsteadiness and non-planarity since the measurements are localized to essentially one point in space and time. Our results are consistent with path-integral Monte Carlo (PIMC)¹⁰ models and the Kerley98

EOS at single-shock pressures less than 1 Mbar and above 2 Mbar but deviate at intermediate pressures; the Ross model does not agree with our data over the entire range under study.

This experiment was performed on LLE's OMEGA laser, a neodymium-doped phosphate glass system that operates with frequency-tripled, 0.35- μm light.¹³ To generate the shock pressures explored in these experiments, laser energies of 440 to 3100 J were delivered using a 3.7-ns-duration square pulse. The laser focal region was smoothed using distributed phase plates (DPP's), producing a uniformly irradiated 800- μm -diam spot. Targets consisted of a z -cut, α -quartz anvil mounted on the upper step of a diamond-turned aluminum pusher that was attached to a copper cell filled with cryogenic deuterium (see Fig. 96.16). A plastic ablator was used to reduce hard-x-ray generation. Three thicknesses were used for the ablator–pusher combination: 20 μm of CH on a 90- to 130- μm Al step (90- μm lower step and 130- μm upper step); 20 μm of CH on a 50- to 85- μm Al step, and 20 μm of CH plus 80 μm of CH-Br (plastic with 2% Br by atomic weight) on a 50- to 85- μm Al step. The quartz anvil was glued to the upper step with a glue thickness of ~ 1 μm and hung over the lower step as shown in Fig. 96.16. The deuterium sample explored in this experiment is trapped within the 35- to 40- μm region between the quartz anvil and the thin Al plate. By observing the solid–liquid

transition in deuterium and using the well-known properties of deuterium on the saturation line,¹⁴ we determined that the deuterium density was 0.174 g/cm³. At this density and at the probe laser wavelength of 532 nm, the index of refraction was calculated to be 1.1381.¹⁴ The density of the quartz was measured to be 2.65 g/cm³. The index of refraction of quartz along its c axis at 532 nm was measured to be 1.547.

The shock diagnostic was a line-imaging velocity interferometer system for any reflector (VISAR),^{15,16} which measures the Doppler shift of a moving reflector. Two VISAR's with different velocity sensitivities were used to resolve 2π phase-shift ambiguities that occur at shock breakout from the aluminum and upon transit of the shock front from deuterium into quartz. The velocity sensitivities for the two VISAR instruments were 6.069 and 14.138 $\mu\text{m}/\text{ns}/\text{fringe}$ for deuterium and 4.465 and 10.400 $\mu\text{m}/\text{ns}/\text{fringe}$ for quartz. Post-processing of the VISAR images can determine the fringe position to $\sim 5\%$ of a fringe; since the measured shock velocities are 25 to 45 $\mu\text{m}/\text{ns}$ in deuterium and 14 to 24 $\mu\text{m}/\text{ns}$ in quartz, multiple fringe shifts allow the precision of the shock-velocity measurement to be $\sim 1\%$. The probe source was an injection-seeded, Q -switched, yttrium–aluminum garnet laser, operating at a wavelength of 532 nm with a pulse length of ~ 25 ns. Streak cameras with temporal windows of ~ 3 ns were used to detect the reflected probe signal. The time resolution of the VISAR and streak camera system was about 40 ps.



E12734

Figure 96.16
Characteristic cryogenic deuterium target design. Dimensions are for one of the three types of target.

A sample VISAR trace is shown in Fig. 96.17(a), and the resulting velocity profile inferred from the fringe positions is given in Fig. 96.17(b). The three clear events observed in these records are marked by fringe (and, hence, velocity) shifts: The first shift represents the velocity jump that occurs when the shock crosses the aluminum–deuterium interface; the second shift, at time t_x , corresponds to the drop in shock velocity as the shock moves across the deuterium–quartz interface. Shock velocities immediately before and after the shock crosses the D_2 –quartz interface are the primary observables used in this work. The third shift is the jump in velocity observed in quartz when the first shock, reverberating in the compressed deuterium gap, catches the leading shock front in quartz.

To extract the velocity profile, we average the phase information at each time over a 20- to 30- μm region. To determine shock velocities at the deuterium–quartz interface, we take linear fits a few hundred picoseconds before and after t_x and extrapolate them to t_x . This eliminates ambiguities due to slight blurring of the measured velocity in a ± 25 -ps time window centered on t_x caused by the resolution of the VISAR and

streak camera system. Figure 96.18 plots the results in terms of the primary experimental observables: the shock speed in deuterium and quartz.

To compare these observations with EOS models it is necessary to know the high-pressure U_s-U_p relation for quartz. This relation was determined by performing extensive laser-driven shock measurements on quartz,¹⁷ complementing data (reported in early Russian work) obtained using nuclear explosives,¹⁸ and found that $U_s = 3.915 + 1.297 U_p$. Taking into account the errors in the fit coefficients, this is in excellent agreement ($\sim 1\%$) with the relation found in the early Russian work ($U_s = 4.200 + 1.280 U_p$)¹⁹ over the range of pressures in our study. Our measurements were performed using impedance matching with an aluminum standard for which we utilized the experimentally derived aluminum Hugoniot rela-

tion given by $U_s(\text{Al}) = 6.541 + 1.158 U_p(\text{Al})$,¹⁹ because quartz and aluminum are closely impedance matched, the release was accurately calculated from the reflected Hugoniot.²⁰ The results change very little—and only then at the very highest pressures—if we instead use a *SESAME* EOS for aluminum.²¹

Silica is known to possess a number of polymorphic phase transitions in the solid regime below 1 Mbar.²² Above ~ 1 Mbar, where silica is a fluid, quartz Hugoniot measurements have shown no indication of a subsequent structural change.¹⁸ Our data begin at ~ 2.5 Mbar and closely follow a linear fit in U_s-U_p .

Using this fit and the impedance-matching conditions at the deuterium–quartz interface, we calculate the reflected shock curves for the different EOS models. These are shown in Fig. 96.18, where the uncertainty in the linear fit to the quartz Hugoniot is the thickness of the thick blue line (for clarity, the PIMC results, which are close to the Kerley98 predictions, are shown as squares). Plotting the data in terms of the experimental observables thus allows uncertainties in the quartz Hugoniot

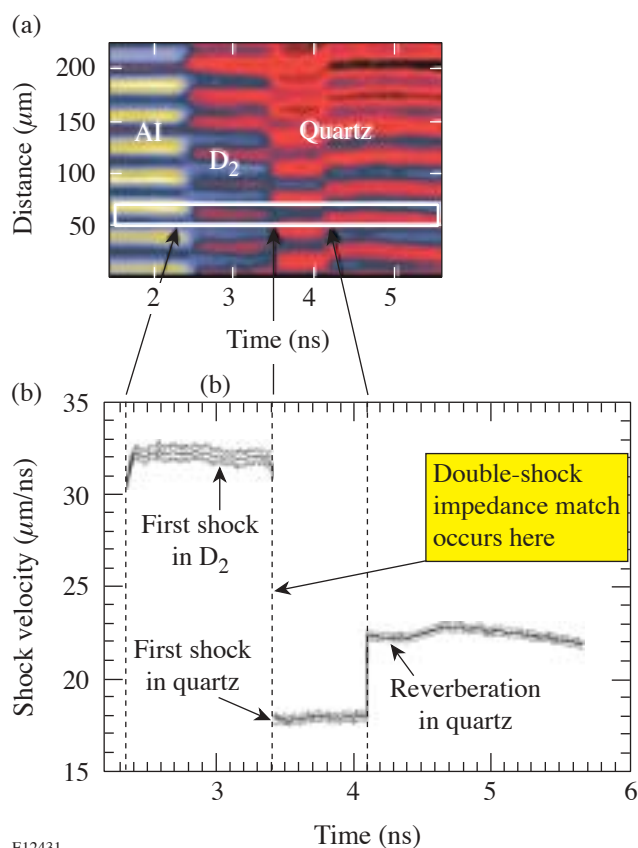


Figure 96.17

(a) Sample VISAR trace showing the signal from the reflecting shock front in deuterium and quartz. (b) Resulting velocity profile extracted from the VISAR trace in (a). Dotted lines above and below the main trace indicate the error at each time step. The shock traverses the deuterium–quartz interface at time t_x .

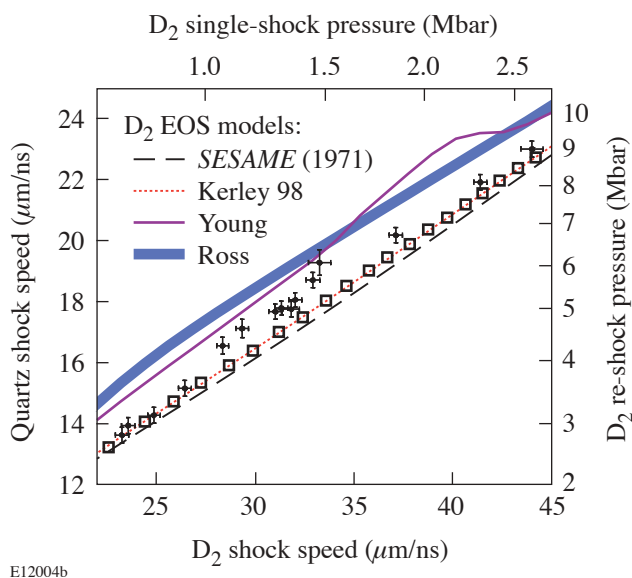


Figure 96.18

Double-shock data for fluid deuterium obtained using an α -quartz anvil (dark circles with error bars). Predictions for different equations of state are shown: *SESAME*⁵ (long dashed), Kerley98⁸ (red dotted), Young⁹ (solid), Ross' linear-mixing model⁷ (thick blue), and PIMC¹⁰ (squares). The measured uncertainty in the quartz Hugoniot is about the thickness of the lines. The estimated D₂ single-shock and re-shock pressures on the top and right axes are based on the PIMC model for D₂ and the measured quartz Hugoniot, respectively.

to be separated from measurement errors in the deuterium re-shock experiments (which are given by the error bars on the data points). We note that the difference in expected quartz shock velocities between the softer Ross model and the stiffer Kerley98 model is close to 10% over much of the range of study. Our experimental precision of $\sim\pm 1\%$ allows us to readily discriminate between these models. The results indicate that double-shock compression of deuterium from single-shock pressures between 0.7 and 2.5 Mbar cannot be adequately described over this range by any of the models shown. Between single-shock pressures of 0.7 and 1.0 Mbar, the PIMC¹⁰ and Kerley98⁸ predictions are consistent with our data; in the regime between 1.0 and 1.3 Mbar the data approach the predictions of the Young model⁹ but disagree with all models between 1.3 and 2.0 Mbar; above 2 Mbar, the results are again consistent with the stiffer PIMC and Kerley98 calculations, while at higher pressures the measurements are in agreement with the stiffer models.

A number of potential systematic effects that could compromise our data have been considered and are addressed below. The steadiness of shock-wave velocities in our experiments varied from shot to shot, depending on the laser drive, ranging from fractions of a percent to several percent over a few nanoseconds. Our new technique of determining shock velocities at essentially a single point in time using continuous measurements is not affected by such variations, unlike the transit-time measurements that were used in the earlier re-shock experiments.² To establish this, we performed extensive hydrodynamic simulations of our experimental arrangement using shock waves with a wide range of unsteadiness—rising and decaying. We saw no deviations from the steady shock case if the velocities were extrapolated to time t_x . This is confirmed experimentally where we observe no difference between the shots that were essentially steady and those that had several-percent unsteadiness.

Shock nonplanarity is also a potential problem, especially for an experiment that requires measurement of a breakout event at spatially separated positions. Since our measurement is performed at a localized point in space, we are not subject to such errors. Nonplanarity could affect our measurements if the wave is incident on the deuterium–quartz interface at an angle large enough to undergo significant refraction. Based on our measurement of the small curvature observed at the deuterium–quartz interface, we infer that the largest incident angles present in our experiments are 3° to target normal. The resulting change in the projected shock speed is less than 0.1% and can be neglected.

X-ray preheating of our target system is a process that would tend to make our data look less compressible. Using an etalon sensitive to motions as low as $0.1\ \mu\text{m}/\text{ns}$, we observed no expansion of the aluminum pusher prior to shock breakout. In addition, for targets shot at similar laser energies, we saw no difference in the results whether we used a $50\text{-}\mu\text{m}$ -thick or $90\text{-}\mu\text{m}$ -thick aluminum pusher. Since the attenuation length for a 1.55-keV x ray (just below the K edge of aluminum) is $10\ \mu\text{m}$, the extra $40\ \mu\text{m}$ of Al would be expected to reduce the x-ray fluence by a factor of 50. The absence of any difference between results from these two targets indicates that x-ray preheat is negligible for these experiments.

In conclusion, we have performed the highest-precision re-shock experiments to date on deuterium shocked to initial pressures between 0.7 and 2.5 Mbar. Below 1 Mbar and above 2 Mbar, the results are in approximate agreement with predictions based on the PIMC and Kerley98 models—models that have near-fourfold compression on the principal Hugoniot—but disagree with these theories between 1 and 2 Mbar. In contrast to earlier re-shock results,² our higher-precision measurements are not consistent with the Ross linear-mixing model. At present, no theory adequately accounts for our observed re-shock results over the entire range under study. We emphasize that there is no model-independent way to compare re-shock measurements with principal Hugoniot measurements since second-shock pressures are affected not only by the density of the first shock but also by the sound speed (or isentropic compressibility) of the compressed states. Given that shock experiments on deuterium above 0.4 Mbar have yielded a wide range of results, the equation of state of hydrogen at megabar pressures and electron-volt temperatures remains an open question. Ultimately a variety of different experimental techniques performed over a broad region of phase space will be required before a consistent picture can emerge.

ACKNOWLEDGMENT

We thank G. I. Kerley, B. Militzer, and D. A. Young for providing model calculations and the LLE Mechanical Engineering, target fabrication, and OMEGA operations staff for their efforts during these experiments. This work was performed under the auspices of the U.S. Department of Energy by LLNL under Contract No. W-7405-ENG-48 and by the University of Rochester under Cooperative Agreement No. DE-FC03-92SF19460.

REFERENCES

1. L. B. Da Silva *et al.*, Phys. Rev. Lett. **78**, 483 (1997); G. W. Collins *et al.*, Science **281**, 1178 (1998); G. W. Collins *et al.*, Phys. Plasmas **5**, 1864 (1998).

2. A. N. Mostovych *et al.*, Phys. Rev. Lett. **85**, 3870 (2000); A. N. Mostovych *et al.*, Phys. Plasmas **8**, 2281 (2001).
3. M. D. Knudson *et al.*, Phys. Rev. Lett. **87**, 225501 (2001); M. D. Knudson *et al.*, Phys. Rev. Lett. **90**, 035505 (2003).
4. S. I. Belov *et al.*, JETP Lett. **76**, 433 (2002).
5. G. I. Kerley, Los Alamos National Laboratory, Report LA-4776 (1972); J. Chem. Phys. **73**, 469 (1980); J. Chem. Phys. **73**, 478 (1980); J. Chem. Phys. **73**, 487 (1980).
6. D. Saumon and G. Chabrier, Phys. Rev. A **46**, 2084 (1992); D. Saumon, G. Chabrier, and H. M. Van Horn, Astrophys. J., Suppl. Ser. **99**, 713 (1995).
7. M. Ross, Phys. Rev. B, Condens. Matter **58**, 669 (1998).
8. G. I. Kerley, Lawrence Livermore National Laboratory, private communication (2002). This model has also been referred to as the *SESAME* model (Ref. 3) but shows softer behavior than the original *SESAME* (Ref. 5) referred to in earlier publications (Ref. 1).
9. D. A. Young, in *Shock Compression of Condensed Matter-1999*, edited by M. D. Furnish, L. C. Chhabildas, and R. S. Hixson (American Institute of Physics, Melville, NY, 2000), pp. 53–56.
10. B. Militzer and D. M. Ceperley, Phys. Rev. Lett. **85**, 1890 (2000); B. Militzer *et al.*, Phys. Rev. Lett. **87**, 275502 (2001).
11. T. J. Lenosky *et al.*, Phys. Rev. B, Condens. Matter **61**, 1 (2000); L. A. Collins *et al.*, Phys. Rev. B, Condens. Matter **63**, 184110 (2001).
12. R. Smoluchowski, Nature **215**, 691 (1967); W. B. Hubbard, Science **214**, 145 (1981); W. B. Hubbard *et al.*, Phys. Plasmas **4**, 2011 (1997); G. Chabrier *et al.*, Astrophys. J. **391**, 817 (1992); G. Chabrier and I. Baraffe, Astron. Astrophys. **327**, 1039 (1997).
13. T. R. Boehly, D. L. Brown, R. S. Craxton, R. L. Keck, J. P. Knauer, J. H. Kelly, T. J. Kessler, S. A. Kumpan, S. J. Loucks, S. A. Letzring, F. J. Marshall, R. L. McCrory, S. F. B. Morse, W. Seka, J. M. Soures, and C. P. Verdon, Opt. Commun. **133**, 495 (1997).
14. P. C. Souers, *Hydrogen Properties for Fusion Energy* (University of California Press, Berkeley, 1986).
15. L. M. Barker and R. E. Hollenbach, J. Appl. Phys. **43**, 4669 (1972).
16. P. M. Celliers *et al.*, Appl. Phys. Lett. **73**, 1320 (1998).
17. D. G. Hicks *et al.*, “Measurements of the Equation of State of Quartz,” in preparation.
18. L. V. Al’tshuler, R. F. Trunin, and G. V. Simakov, Izv. Acad. Sci. USSR Phys. Solid Earth, No. 1, 657 (1965); R. F. Trunin *et al.*, Izv. Acad. Sci. USSR Phys. Solid Earth, No. 1, 8 (1971); R. F. Trunin, Phys.-Usp. **37**, 1123 (1994).
19. R. F. Trunin, ed. *Experimental Data on Shock Compression and Adiabatic Expansion of Condensed Matter* (Russian Federal Nuclear Center–VNIIEF, Sarov, 2001).
20. R. F. Trunin, *Shock Compression of Condensed Materials* (Cambridge University Press, Cambridge, England, 1998).
21. The *SESAME* table for aluminum compared in this case was #3718, given in S. P. Lyon and J. D. Johnson, Los Alamos National Laboratory, Los Alamos, CA, Report LA-UR-92-3407 (1992). For our analysis, differences between the various *SESAME* tables for aluminum are negligible.
22. See, for example, J. A. Akins and T. J. Ahrens, Geophys. Res. Lett. **29**, 31-1 (2002) and references therein.